Chinese Medical Journal®

Necroptosis was found in a rat ischemia/reperfusion injury flap model

Hao Liu[1,2], Ming-Zi Zhang[1], Yi-Fang Liu[3], Xin-Hang Dong[1], Yan Hao[1], You-Bin Wang[1]

[1]Department of Plastic Surgery, Peking Union Medical College Hospital, Beijing 100005, China;
[2]Chinese Academy of Medical Sciences & Peking Union Medical College, Beijing 100005, China;
[3]International Education College, Beijing Vocational College of Agriculture, Beijing 100012, China.

Abstract

Background: Necroptosis is a new form of cell death that has been identified as a third pathway causing cell death. In this study, necrostatin-1 (Nec-1) was used to determine whether necroptosis exists in a rat ischaemia/reperfusion injury flap model.

Methods: In this study, twenty male Sprague-Dawley rats were divided randomly into two groups: a control group (CTL group) and a Nec-1 group. Each abdominal skin flap underwent 3 h of ischaemia and then reperfusion. Fifteen minutes before and after reperfusion, phosphate buffer saline (PBS) was administered intraperitoneally to the CTL group, while Nec-1 was administered intraperitoneally to the Nec-1 group. Twenty-four hours after reperfusion, the whole flap was divided equally into 54 sections. Flap blood perfusion was measured. One sample was taken randomly from each row. Morphological changes, apoptosis, receptor-interacting protein-1 (RIP-1) expression and caspase-3 activity were observed and detected. The measurements between the two groups were compared with the independent *t*-test, and a *P* value of <0.05 was considered statistically significant.

Results: Compared to flaps in the CTL group, flaps in the Nec-1 group showed longer survival rates, better blood perfusion and less inflammatory infiltration. The total flap area considered to have survived was $70.88 \pm 10.28\%$ in the CTL group, whereas $80.56 \pm 5.40\%$ of the area was found to be living in the Nec-1 group (Nec-1 vs. CTL, $t=-2.624$, $P<0.05$). For some rows, there were significant differences in cell apoptosis between the two groups, the apoptosis index (AI) in rows "9 cm", "7 cm", "6 cm" and "5 cm" was significantly lower in the Nec-1 group than that in the CTL group (Nec-1 vs. CTL, $P<0.05$). RIP-1 expression was much lower in the Nec-1 group than that in the CTL group in rows "5 cm" to "9 cm" (Nec-1 vs. CTL, $P<0.05$). No significant differences in caspase-3 activity were found.

Conclusion: According to the results, necroptosis was present in a rat abdominal ischaemia/reperfusion injury flap model.

Keywords: Necrostatin-1; necroptosis; cell death; ischaemia/reperfusion injury; skin flap

Introduction

Cell death is a major physiological or pathological phenomenon that occurs when a biological cell ceases to carry out its functions. The classic forms of cell death include necrosis and apoptosis. Necrosis is a form of cell injury that results in the premature death of cells in living tissue by autolysis.[1] Apoptosis is a process of programmed cell death that occurs in multicellular organisms.[2] Recently, a novel type of cell death has been observed and named necroptosis, which is a programmed form of necrosis or inflammatory cell death. Conventionally, the classic cell death pathway (necrosis) is usually related to unprogrammed cell death caused by cellular damage instead of programmed cell death, which occurs via apoptosis. Necroptosis is a well-defined viral defence mechanism that allows the cell to undergo "cellular suicide" in a caspase-independent fashion in the presence of viral caspase inhibitors.[3] In Degterev *et al*'s study,[4] the researchers showed that necroptosis is characterized by necrotic cell death morphology and autophagy activation. Necrostatin-1 (Nec-1) was also identified as a specific and potent small molecule inhibitor that blocks a critical step in necroptosis.[4]

Ischaemia/reperfusion (I/R) injury is the tissue damage caused when blood returns to a tissue after a period of ischaemia. In I/R injury, classic forms of cell death occur. In recent studies, necroptosis was found in myocardial,[5] retinal[6] and renal[7] I/R injury. In plastic surgery, it is widely accepted that I/R injury is a critical factor in flap failure, while cell death is an important feature of the I/R process.[8,9] In the I/R skin flap model, there is no evidence

Access this article online

Quick Response Code:

Website: www.cmj.org

DOI: 10.1097/CM9.0000000000000005

Correspondence to: Dr. You-Bin Wang, Department of Plastic Surgery, Peking Union Medical College Hospital, Beijing 100005, China
E-Mail: wybenz@sina.com

Chinese Medical Journal 2019;132(1)

Received: 29-10-2018 **Edited by:** Yuan-Yuan Ji

of whether necroptosis exists. In this study, Nec-1 was used to evaluate whether necroptosis occurs in a rat abdominal I/R skin flap model.

Methods

Animals and groups

All protocols were approved by the Committee on Animal Rights Protection of Peking Union Medical College Hospital and were in accordance with the National Institutes of Health guidelines for the care and use of laboratory animals. In this study, 280 to 320 g adult male Sprague-Dawley (SD) rats were used. Before and after surgery, each rat was housed in a comfortable individual cage at 22–25 °C with adequate food and drink and a 12-h light-dark cycle.

Before the operation, 20 qualified laboratory SD rats were randomly divided into two groups: a control group (CTL) and a Nec-1 group (Nec-1).

Surgical procedure

An extended epigastric adipocutaneous flap (6 cm × 9 cm) was placed over the abdomen of each rat.[10] The left superficial epigastric artery and vein were ligated, and the right side was retained as the pedicle. Flap ischaemia was induced for 3 h in both groups by clamping the right superficial epigastric artery with a microvascular clamp. Then, the flap was resutured with a 0.1-mm-thick silicone sheet to prevent neovascularization from the wound bed. Fifteen minutes before and after removing the clamp, phosphate buffer saline (PBS) (200 μL) was administered intraperitoneally to the CTL group, while Nec-1 (1.65 mg/kg in 200 μL total volume)[7] was administered intraperitoneally to the Nec-1 group. Reperfusion was initiated by removing the clamp (Figure 1).

Preparation for sampling

To evaluate the histological and morphological changes, whole abdominal skin flaps were divided equally into 54 sections (6 lines and 9 rows) before sampling (Figure 2). Twenty-four hours after reperfusion, samples (1 cm × 1 cm) were taken randomly from sections "01" to "06" in each row. Nine samples were taken for further analyses, including haematoxylin and eosin (H&E) staining, TdT-mediated dUTP-X nick end labelling (TUNEL) staining, electron microscope examination, immunohistochemical (IHC) staining and an enzyme-linked immunosorbent assay (ELISA) for caspase-3 activity detection.

Flap survival rate and blood perfusion evaluation

Skin flap survival rates and blood perfusion were evaluated 24 h after reperfusion by a laser Doppler flowmeter (LDF, Perimed AB, Stockholm, Sweden) and laser speckle contrast analysis (LSCA, Perimed AB, Stockholm, Sweden). At an environmental temperature of 20 to 25°C, the rats were anaesthetized and secured on the operating table to expose the entire flap. Then, LDF was used to measure the capillary blood flow in the dermal skin layer of the rats (distance between the skin flap and sensor: 20 cm). Perfusion in the necrotic and surviving flap areas was evaluated automatically by delineating the specific area of the image with LSCA.

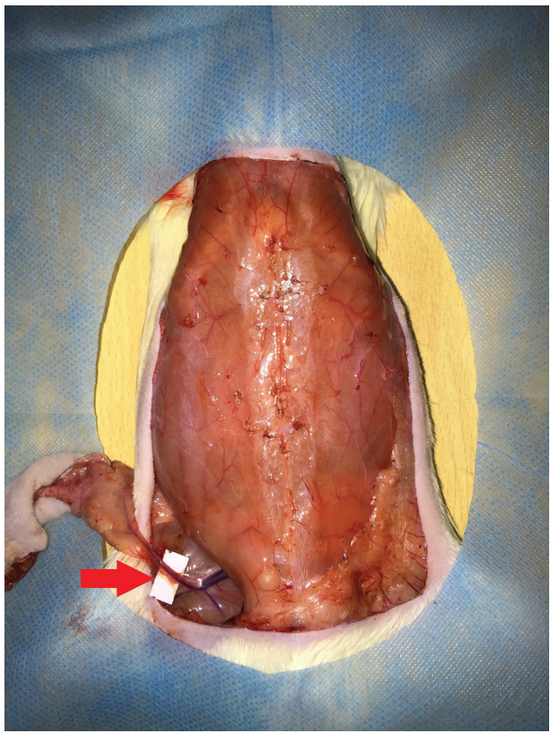

Figure 1: An extended epigastric adipocutaneous flap (6 cm × 9 cm) was raised over the abdomen in each rat. The left superficial epigastric artery and vein were ligated (red arrow). Flap ischemia of 3 h was induced in both groups by clamping the right superficial epigastric artery with a microvascular clamp.

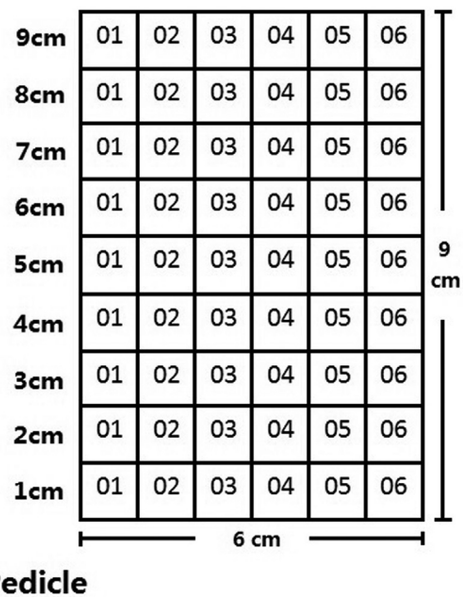

Figure 2: Fifty-four sections of the abdominal skin flap before sampling. There are 6 lines and 9 rows in each flap. In each row, there are 6 flap sections (1 cm × 1 cm) numbered "01" to "06". When sampling, one number was randomly chosen as the sample.

H&E staining

For H&E staining, the specimens were fixed in formalin for at least 24 h. After the tissues were paraffin-embedded, sectioned and mounted on a slide, they were stained with H&E for histological examination.

TUNEL staining and apoptosis index evaluation

TUNEL staining was performed using an *In Situ* Cell Death Detection Kit (Roche, Basel, Switzerland). All protocols were conducted according to the manufacturer's instructions. For quantitation analysis, TUNEL-positive cells in 3 different slide fields from different skin flap tissues were counted and presented as an apoptosis index (AI).

Transmission electron microscopy observation

Specimens were fixed with glutaraldehyde fixing solution and were made into slides for electron microscope observation by the Institute of Basic Medical Sciences Chinese Academy of Medical Sciences & School of Basic Medicine Peking Union Medical College. Electron microscope: JEM-1400 (JEOL, Japan). Acceleration voltage: 80 kV.

IHC staining

The paraffin slides were deparaffinized in xylene and rehydrated with various concentrations of ethanol. Then, 3% H_2O_2 was used to deactivate endogenous oxidases. The slides underwent antigen retrieval and blocking with goat serum. Then, the slides were incubated overnight at 4°C with an receptor-interacting protein-1 (RIP-1) antibody (1:50 dilution, ZSGB-BIO, Beijing, China). After rinsing with PBS, the samples were incubated with a horseradish peroxidase-conjugated secondary antibody (ZSGB-BIO, Beijing, China). Then, the samples were flushed with PBS, stained with DAB and counterstained with haematoxylin. A brown colour implied the presence of antibody bound to antigen and was detected by a light microscope (Olympus Corporation, Tokyo, Japan) with a computer-controlled digital camera and imaging software.

Caspase-3 activity assay

Caspase-3 activity was detected using a Fluorometric Assay Kit (BioVision Research Products, Mountain View, CA, USA). Briefly, 40 mg of tissue was homogenized in 2× reaction buffer and incubated for 1 h at 37°C with caspase-3 substrate (DEVD-APC) (1 mmol/L). Substrate cleavage was measured with a spectrofluorometer at 400 nm.

Western blotting analysis

Protein was extracted from 50-mg samples with a cell lysis kit (Bio-Rad Laboratories, Hercules, CA, USA). The samples were incubated in buffer (246 μL lysis buffer, 1.25 μL phosphatase inhibitor, 0.25 μL protease inhibitor, and 2.5 μL PMSF) on ice for 10 min and then centrifuged. For Western blotting, equal amounts of protein supernatant (60 μg) were separated by 10% SDS-PAGE and transferred onto nitrocellulose membranes for immunoblotting. The membranes were blocked with blocking buffer (Li-cor, Lincoln, NE, USA) for 2 h and then incubated with either anti-CKLF-1 (1:100, Peking University Center for Human Disease Genomics, Peking University, Beijing, China), anti-IL-6 (1:500, Abcam, Cambridge, UK), anti-IL-8 (1:500, Abcam), anti-IL-18 (1:500, Abcam), anti-TGF-β (1:500, Abcam), or anti-β-actin (1:2000, Santa Cruz Biotechnology, Dallas, TX, USA) antibodies for 12 h at 4°C. The membranes were incubated with secondary antibodies (Li-cor, Lincoln, NE) at a 1:10,000 dilution in the dark for 1 h at room temperature and then detected with a double colour infrared laser imaging system (Odyssey, Li-cor, Lincoln, NE, USA).

Statistical analysis

The measurements in this study were described as mean ± standard error (SE), and all their distributions levels were found to comply with Gaussian distributions ($\alpha = 0.05$) with analysis of skewness and kurtosis. Differences in numeric variables between the two groups were analyzed by the independent sample *t*-test with 2-tailed *P* values. The *P* value of <0.05 was considered statistically significant. All the statistical calculations were performed using SPSS v.22 (SPSS Inc., USA).

Results

Flap survival and perfusion

The flap survival rate was measured by blood distribution area, and flap perfusion was evaluated by blood flow (Figure 3A); their comparisons are presented in Figure 3B and 3C. The total flap area considered to have survived was 70.88 ± 10.28% in the CTL group, whereas 80.56 ± 5.40% (Nec-1 vs. CTL, $t = -2.624$, $P < 0.05$) of the area was found to be living in the Nec-1 group. The average blood perfusion in the CTL group was 52.45 ± 8.63 PU ml·100 g^{-1}·min^{-1}, which was significantly less (Nec-1 vs. CTL, $t = -3.475$, $P < 0.01$) than the perfusion in the Nec-1 group (64.06 ± 6.10 PU ml·100 g^{-1}·min^{-1}).

Histological analysis

H&E-stained tissue slides were used to assess inflammatory infiltration caused by I/R injury (Figure 4). In row "1 cm" to row "5 cm", less inflammatory infiltration was found in each group. However, more inflammatory cells were found in the dermal and subcutaneous layers of the skin tissue from row "6 cm" to row "9 cm" in the CTL group than in the Nec-1 group.

AI evaluation

Apoptotic cells were observed with TUNEL staining (Figure 5). The number of apoptotic cells increased gradually from row "1 cm" to row "9 cm". The AI in rows "9 cm", "7 cm", "6 cm" and "5 cm" was significantly lower in the Nec-1 group than in the CTL group. The AI data are shown in Table 1.

Electron microscopy observation

An electron microscope was used to identify the morphological changes of apoptotic cells. The morpho-

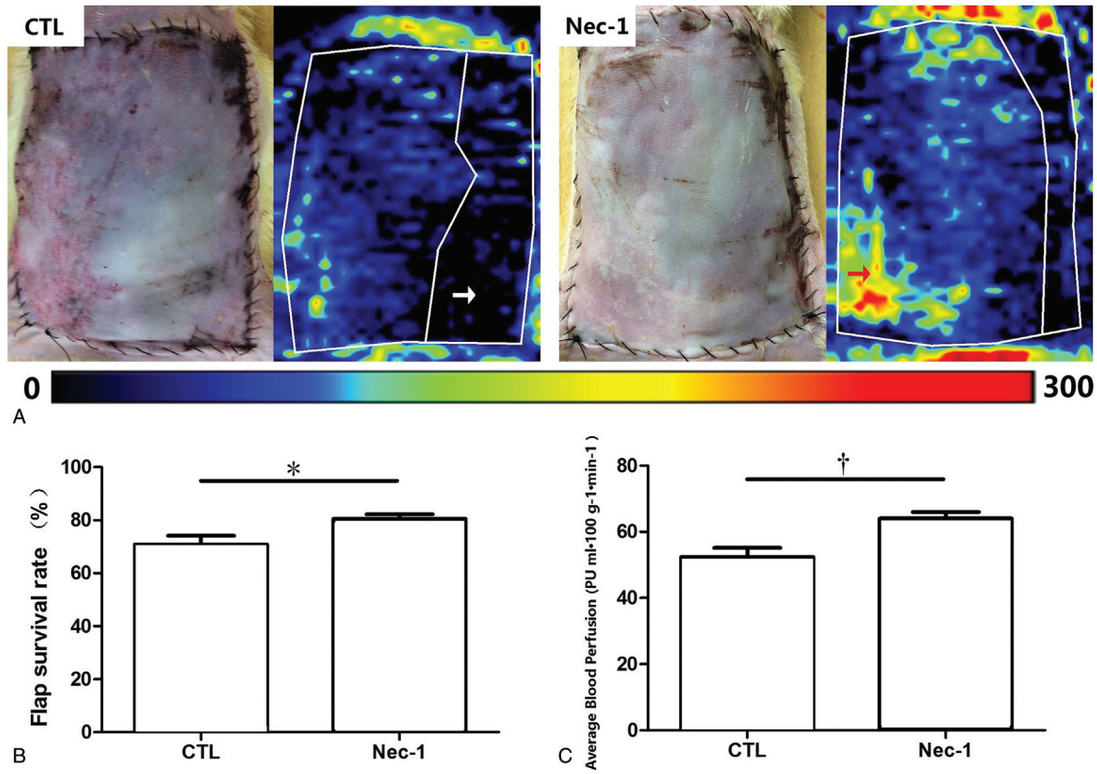

Figure 3: The condition of the abdominal skin flaps. The white arrow pointing to black zones presents the lowest blood perfusion. The red arrows pointing to red, yellow and the adjacent blue areas present surviving areas with rich blood flow. (A) Representative photographs of abdominal skin flap microcirculation in both groups. (B) The flap survival rate of the total flap area. Flap survival rates were higher in the Nec-1 group. (C) The average blood perfusion of total skin flaps. The average blood perfusion of the total flap was greater in the Nec-1 group. The values are expressed as mean ± standard error (n = 10 for each group; $^{*}P < 0.05$, $^{\dagger}P < 0.01$). Nec-1: Necrostatin-1 group; CTL: Control group.

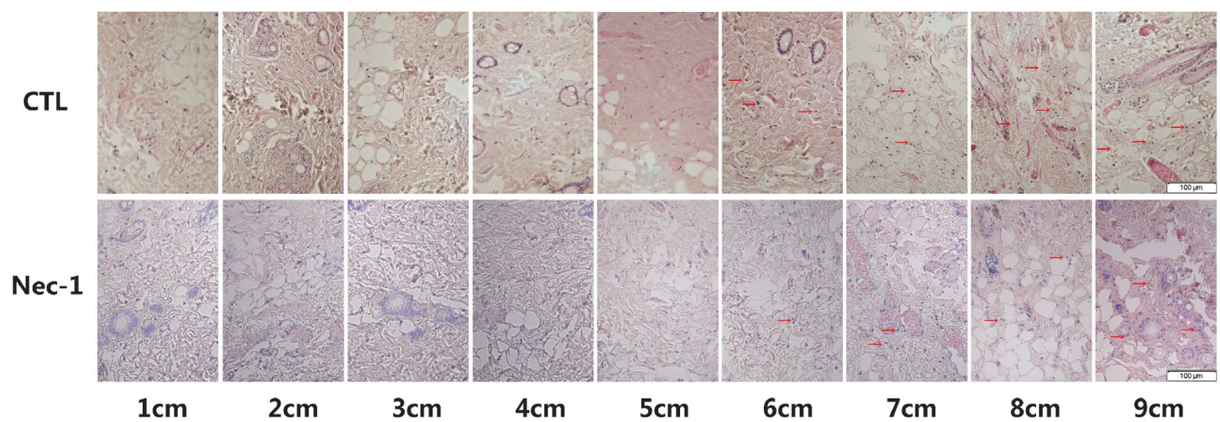

Figure 4: The histological observation of flap tissue by H&E staining in both groups. More inflammatory cells (red arrow) from row "6 cm" to "9 cm" were found in the CTL group than in the Nec-1 group. Inflammatory cells were less from row "1 cm" to "5 cm" in both groups (Original magnification ×200).

logical characteristics of apoptotic cells include nuclei with chromatin pyknosis and clustering on the inner border of the karyotheca, as well as condensed cytoplasm with many vacuoles. The results showed that typical apoptotic cells showed up in row "3 cm" in the CTL group while they appeared in row "7 cm" in the Nec-1 group (Figure 6).

Immunohistochemical studies for RIP-1

Immunohistochemical specimen staining for each group is shown in Figure 7. The results showed that in the CTL group, RIP-1 expression was higher in rows "5 cm" to "9 cm". In the Nec-1 group, RIP-1 expression was higher in rows "8 cm" to "9 cm" (Figure 7).

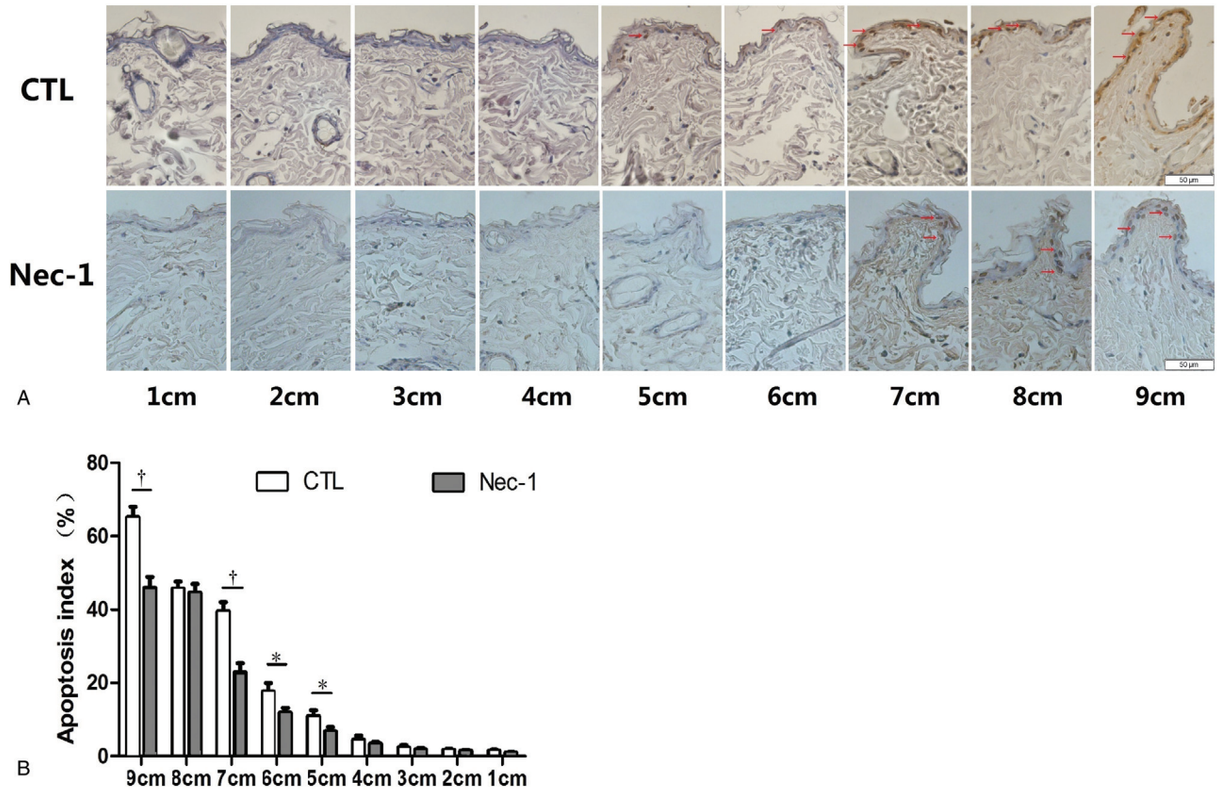

Figure 5: The results of TUNEL staining and the apoptosis index in each group. (A) The evaluation of apoptotic cells (red arrow) by TUNEL staining (Original magnification ×400). (B) The apoptosis index of all groups. The number of apoptotic cells increased gradually from row "1 cm" to row "9 cm". The values are expressed as mean ± standard error ($n = 10$ for each group; $^{*}P < 0.05$, $^{\dagger}P < 0.001$).

Table 1: The data of apoptosis index in each row of the Nec-1 and CTL groups ($n = 10$ for each group)

Row	Apoptosis index (%)		*t*	*P*
	CTL group	Nec-1 group		
1 cm	1.4790 ± 1.1457	0.9770 ± 0.6569	1.202	0.245
2 cm	1.7460 ± 0.9733	1.4900 ± 0.8758	0.618	0.544
3 cm	2.3940 ± 2.0878	1.8060 ± 1.5439	0.716	0.483
4 cm	4.4730 ± 3.6407	3.4420 ± 1.3813	0.837	0.413
5 cm	10.9830 ± 4.9313	6.7410 ± 3.9719	2.119	0.048
6 cm	17.6340 ± 7.3138	11.8860 ± 4.0819	2.170	0.044
7 cm	39.5730 ± 7.8457	22.9160 ± 7.7604	4.773	0.000
8 cm	45.7170 ± 5.9905	44.6340 ± 7.4147	0.359	0.724
9 cm	65.2390 ± 8.8989	45.9240 ± 9.3198	4.740	0.000

Nec-1: Necrostatin-1 group; CTL: Control group.

Caspase-3 activity assay

In both groups, caspase-3 activity increased gradually from row "1 cm" to "9 cm". However, there was no significant difference between the CTL group and the Nec-1 group in the same specimen rows (Figure 8). The caspase-3 activity data are shown in Table 2.

RIP-1 protein expression

RIP-1 protein expression in the skin tissues from the two groups was visualized by Western blotting (Figure 9). RIP-1 expression was much lower in the Nec-1 group than in the CTL group in rows "5 cm" to "9 cm". The data of RIP-1 expression are shown in Table 3.

Discussion

Cell death is a major physiological or pathological phenomenon that has been researched for many years. Traditionally, there are two main forms of cell death, necrosis and apoptosis.[11] Necrosis is a form of cell injury resulting in the premature death of cells in living tissue by autolysis,[1] which is caused by external cell or tissue

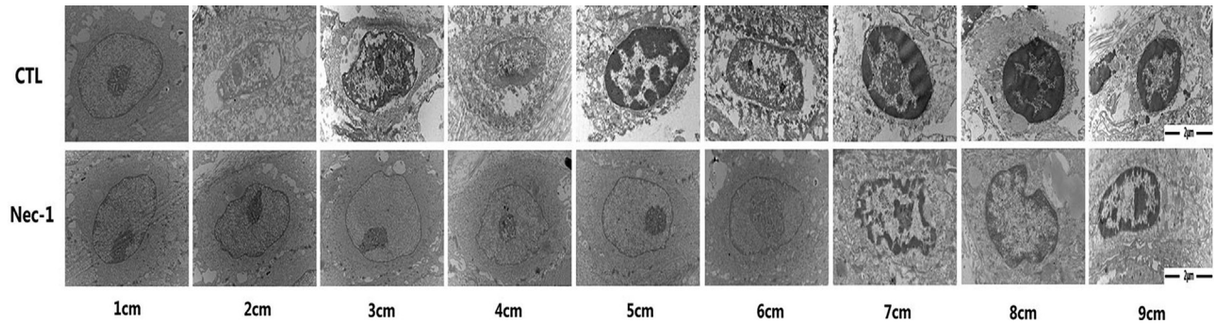

Figure 6: The morphology of cells in each row of each group. All of the observed apoptotic cells showed cell body shrinkage, cytoplasm density increase and chromatin condensation, but the nuclear membrane, plasma membrane and organelles were intact. The results showed that typical apoptotic cells showed up in row "3 cm" in the CTL group, while they appeared in row "7 cm" in the Nec-1 group (Original magnification ×12,000).

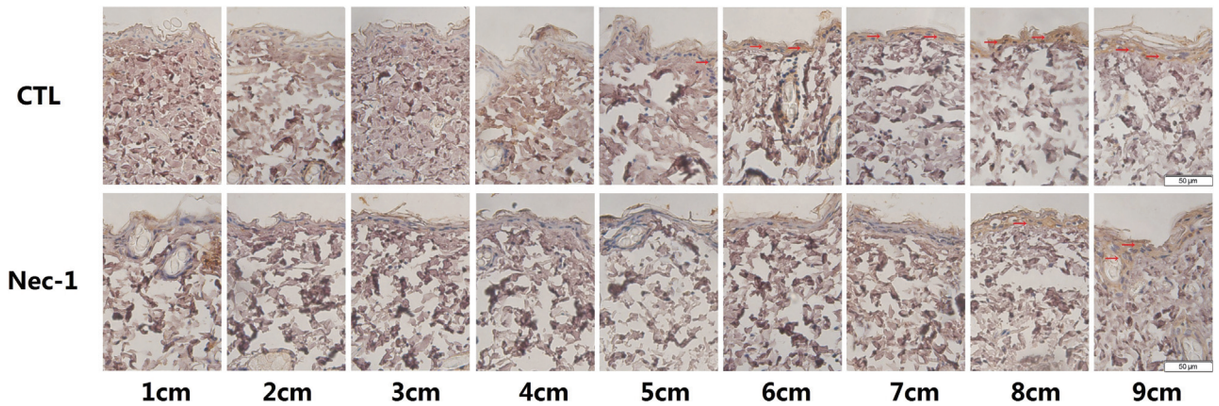

Figure 7: Representative micrographs of flap tissue for RIP-1 (Immunohistochemical staining, original magnification ×400). Brown staining indicates positive expression areas (red arrow), and the shade of color represents the expression level of the target protein. In the CTL group, RIP-1 expression was gradually increased from row "5 cm" to "9 cm" (+∼+++). RIP-1 expression was higher in row "8 cm" to "9 cm" (+∼++) in the Nec-1 group.

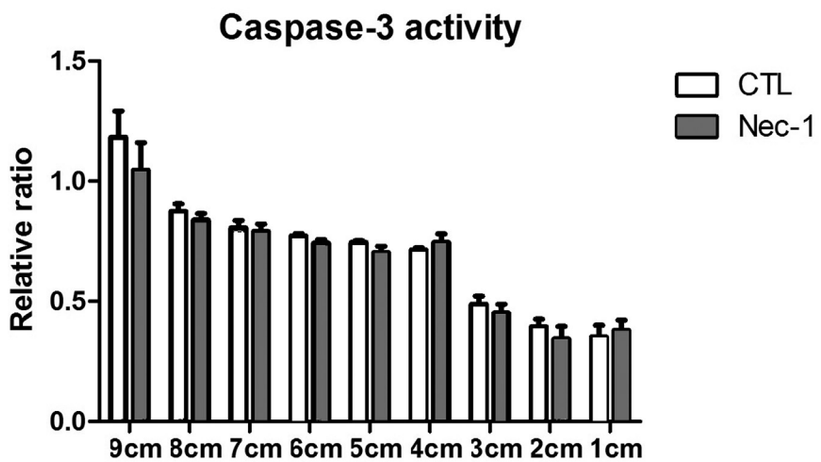

Figure 8: Caspase-3 activity in each row of each group. Caspase-3 activity gradually decreased from row "9 cm" to "1 cm". However, there was no significant difference between the CTL group and Nec-1 group in the same row.

Table 2: The data of caspase-3 activity in each row of the Nec-1 and control groups (n=10 for each group)

	Caspase-3 activity relative ratio			
Row	CTL group	Nec-1 group	*t*	*P*
1 cm	0.3525±0.1515	0.3791±0.1363	−0.414	0.684
2 cm	0.3945±0.0967	0.3427±0.1663	0.852	0.405
3 cm	0.4875±0.1104	0.4508±0.1171	0.892	0.480
4 cm	0.7148±0.0277	0.7454±0.1112	−0.845	0.409
5 cm	0.7451±0.0235	0.7031±0.0842	1.519	0.146
6 cm	0.7721±0.0291	0.7425±0.0453	1.737	0.099
7 cm	0.8052±0.0990	0.7903±0.0989	0.334	0.743
8 cm	0.8748±0.0968	0.8382±0.0853	0.896	0.382
9 cm	1.1830±0.3455	1.0457±0.3646	0.864	0.399

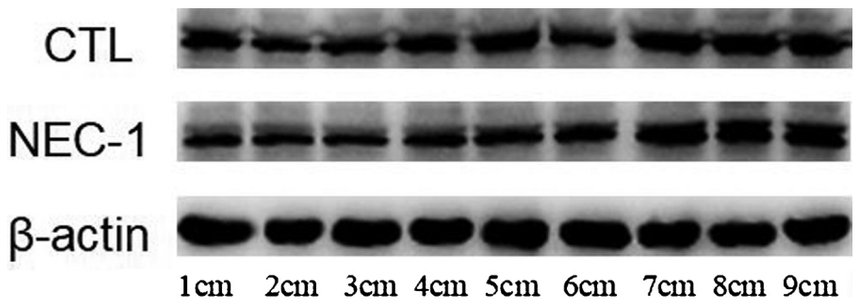

Figure 9: The protein expression of RIP-1 in skin tissues of the two groups. In Nec-1 group, the expression of RIP-1 was much lower than that in CTL group in row "5 cm" to "9 cm".

Table 3: The data of RIP-1 expression in each row of the Nec-1 and control groups (n=10 for each group)

	RIP-1 expression			
Row	CTL group	Nec-1 group	*t*	*P*
1 cm	0.8960±0.0367	0.9608±0.0252	−2.521	0.065
2 cm	0.8820±0.0780	0.9748±0.1029	−1.244	0.281
3 cm	0.8404±0.0210	0.9358±0.0734	−2.163	0.097
4 cm	0.9896±0.0493	1.0393±0.0081	−1.725	0.161
5 cm	0.8795±0.0446	1.1450±0.1110	−3.842	0.018
6 cm	0.9805±0.0555	1.2071±0.0618	−4.723	0.009
7 cm	1.0337±0.0174	1.2828±0.1223	−3.493	0.025
8 cm	1.0967±0.0381	1.3237±0.0894	−4.044	0.016
9 cm	1.1411±0.0374	1.3529±0.0317	−5.523	0.005

factors, such as toxins, infection and trauma. There are 6 distinctive morphological patterns of necrosis: coagulative necrosis, liquefactive necrosis, gangrenous necrosis, caseous necrosis, fat necrosis, and fibrinoid necrosis.[12] In contrast, apoptosis is a precisely controlled and regulated process of programmed cell death that occurs in multicellular organisms.[2] In contrast to necrosis, apoptotic bodies emerge during the apoptosis process, and these bodies can be recognized, engulfed and removed quickly by phagocytic cells before the cell contents spill out into the extracellular environment and cause damage. Cell death ends with many morphological changes, including blebbing, cell shrinkage, nuclear fragmentation, chromosomal DNA fragmentation, chromatin condensation and global mRNA decay.[13]

Recently, a novel type of cell death was observed and named necroptosis. The discovery of necroptosis demonstrated that necrosis could be performed in a programmed fashion. Unlike necrosis, cell membrane permeabilization is highly regulated during the necroptosis process. Some of the mechanisms and components of the signalling pathway are still unknown. Vanden *et al*'s study[3] demonstrated that extrinsic stimuli act on the TNF receptor TNF-α, and the signals recruit the TNF receptor-associated death domain (TRADD), which in turn

activates RIP1 and leads to necrosome formation. Then, the necrosomes activate MLKL, which is a pro-necroptotic protein that initiates the necrosis phenotype by inserting itself into organelle membranes and the plasma membrane; this process then leads to the exclusion of cellular contents from the extracellular space.[14,15] In this case, RIP-1 plays a paramount role in starting the necroptosis process in which caspase-3, a key apoptosis-dependent factor, is not involved. Moreover, Degterev *et al*[4] also noted a specific and potent small molecule inhibitor of necroptosis, Nec-1, which blocks a critical step in the necroptosis process.

I/R injury is the tissue damage caused when blood returns to tissues after a period of ischaemia. In organ transplantation, I/R injury can occur when blood returns to a tissue for the first time. The worst outcome of I/R injury is cell death. Studies have demonstrated that cell apoptosis and necrosis occur during the I/R process. Some researchers have also found necroptosis in I/R injuries. Liu *et al*[5] found a protective effect of heat shock protein 70 against necroptosis in myocardial I/R injury. These researchers identified RIP-1 as a necroptosis marker. Necroptosis has also been found in I/R injuries in the retina and kidney. Gao *et al*'s study of the retina[6] not only reported that necroptosis existed during I/R injury but also that necroptotic cell death was executed by an ERK1/2-RIP3 pathway in the early stages after I/R injury in retinal ganglion cells. In addition, renal research from Linkermann *et al*[7] showed that RIP-1 played an important role in mediating necroptosis and contributing to renal I/R injury. In plastic surgery, there are many reasons for flap failure, and I/R injury is an important one. However, there is no evidence regarding whether necroptosis exists in skin flap I/R injury. Therefore, our study aimed to determine whether necroptosis was present using the necroptosis-specific inhibitor Nec-1.

In our study, the results showed that flaps in the Nec-1 group showed a larger flap survival area and better blood perfusion. To evaluate the histological and morphological changes, whole flaps were divided equally into 54 sections (6 lines and 9 rows) for sampling. Each sample (1 cm × 1 cm) was taken randomly from sections "01" to "06" in each row for H&E, TUNEL and IHC staining, electron microscopy and an ELISA of caspase-3 activity. According to H&E staining, inflammatory infiltration was reduced from row "9 cm" to "1 cm". Pasparakis *et al's* review[16] concluded that there was a close relationship between necroptosis and inflammation. Kaczmarek *et al*[17] also mentioned that I/R injury provoked a strong inflammatory response, which might be triggered by necroptotic cells.

In Mehta *et al's* study,[18] early necroptotic cells showed morphological changes similar to apoptotic cells and ended up with the morphological appearance of necrotic cells. The TUNEL staining and AI results showed that the number of apoptotic cells decreased gradually from row "9 cm" to "1 cm". There were significant differences between the CTL group and the Nec-1 group in rows "9 cm", "7 cm", "6 cm" and "5 cm". In these rows, there were fewer TUNEL-positive cells in the Nec-1 group than those in the CTL group, which indicated that some TUNEL-positive cells caused by necroptosis might be inhibited by Nec-1. According to the electron microscopy results, the apoptotic cells showed cell body shrinkage, increased cytoplasm density and chromatin condensation, but the nuclear membrane, plasma membrane and organelles were intact. The results showed that typical apoptotic cells appeared in row "3 cm" in the CTL group; however, they appeared in row "7 cm" in the Nec-1 group. RIP-1 plays a key role in necroptosis. According to IHC staining, RIP-1 expression increased gradually in rows "5 cm" to "9 cm" (+ to +++) in the CTL group, whereas RIP-1 expression was higher in rows "8 cm" to "9 cm" (+ to ++) in the Nec-1 group. By analysing the AI and IHC staining results, we concluded that necroptotic cells might commonly exist in rows "5 cm" to "9 cm" but primarily exist in rows "7 cm" to "9 cm".

Necroptosis is a well-defined viral defence mechanism that allows cells to undergo "cellular suicide" in a caspase-independent fashion in the presence of viral caspase inhibitors.[3] Caspase-3 plays an irreplaceable role in facilitating the apoptosis process. The caspase-3 activity results showed that there were no significant differences for the same rows between the CTL group and Nec-1 group, which confirmed the caspase-independent characteristic of necroptosis.

Based on all of the above results, necroptosis was found in a rat abdominal skin flap model of I/R injury. In addition, this study showed the morphological changes of cells in different positions in an I/R skin flap. In this case, a new form of cell death was found in skin flaps with I/R injury, which will likely contribute to new research interest in flap I/R injury.

In conclusion, in a rat abdominal skin flap model of I/R injury, a new form of cell death called necroptosis was found. The necroptotic cells were commonly distributed in the flap area distant from the pedicle.

Acknowledgements

None.

Funding

This study was supported by a grant of National Natural Science Foundation of China (No. 81471885).

Conflicts of interest

All the authors do not have any possible conficts of interest.

Author contributions

Wang YB conceived the study. Dong XH, Hao Y and Liu YF were responsible for data management and statistical analyses. All authors were responsible for the interpretation of the data. Zhang MZ and Liu H did the experiment and wrote the report, and all authors read and approved the final manuscript.

References

1. Proskuryakov SY, Konoplyannikov AG, Gabai VL. Necrosis: a specific form of programmed cell death? Exp Cell Res 2003;283:1–16. doi: 10.1016/S0014-4827(02)00027-7.
2. Green, Douglas. Means to an End: Apoptosis and other Cell Death Mechanisms. Cold Spring Harbor, NY: Cold Spring Harbor Laboratory Press. ISBN 978-0-87969-888-1.
3. Vanden Berghe T, Linkermann A, Jouan-Lanhouet S, Walczak H, Vandenabeele P. Regulated necrosis: the expanding network of non-apoptotic cell death pathways. Nat Rev Mol Cell Biol 2014;15:135–147. doi: 10.1038/nrm3737.
4. Degterev A, Huang Z, Boyce M, Li Y, Jagtap P, Mizushima N, et al. Chemical inhibitor of nonapoptotic cell death with therapeutic potential for ischemic brain injury. Nat Chem Biol 2005;1:112–119. doi: 10.1038/nchembio711.
5. Liu X, Zhang C, Zhang C, Li J, Guo W, Yan D, et al. Heat shock protein 70 inhibits cardiomyocyte necroptosis through repressing autophagy in myocardial ischemia/reperfusion injury. In Vitro Cell Dev Biol Anim 2016;52:690–698. doi: 10.1007/s11626-016-0039-8.
6. Gao S, Andreeva K, Cooper NG. Ischemia-reperfusion injury of the retina is linked to necroptosis via the ERK1/2-RIP3 pathway. Mol Vis 2014;20:1374–1387.
7. Linkermann A, Brasen JH, Hummerkus N, Liu S, Huber TB, Kunzendorf U, et al. Rip1 (receptor-interacting protein kinase 1) mediates necroptosis and contributes to renal ischemia/reperfusion injury. Kidney Int 2012;81:751–761. doi: 10.1038/ki.2011.450.
8. Wang WZ, Baynosa RC, Zamboni WA. Update on ischemia-reperfusion injury for the plastic surgeon: 2011. Plast Reconstr Surg 2011;128:685e–692e. doi: 10.1097/PRS.0b013e318230c57b.
9. van den Heuvel MG, Buurman WA, Bast A, van der Hulst RR. Review: ischaemia-reperfusion injury in flap surgery. J Plast Reconstr Aesthet Surg 2009;62:721–726. doi: 10.1016/j.bjps.2009.01.060.
10. Zhao L, Wang YB, Qin SR, Ma XM, Sun XJ, Wang ML, et al. Protective effect of hydrogen-rich saline on ischemia/reperfusion injury in rat skin flap. J Zhejiang Univ Sci B 2013;14:382–391. doi: 10.1631/jzus.B1200317.
11. Hotchkiss RS, Strasser A, Mc Dunn JE, Swanson PE. Cell death. N Engl Med 2009;361:1570–1583. doi: 10.1056/NEJMra0901217.
12. Kumar V, Abbas AK, Aster JC, Fausto N. Robbins and cotran pathologic basis of disease (8th ed). Philadelphia, PA: Saunders/Elsevier: 12–41. ISBN 1416031219.
13. Majno G, Joris I. Apoptosis, oncosis, and necrosis. An overview of cell death. Am J Pathol 1995;146:3–15.
14. Wang H, Sun L, Su L, Rizo J, Liu L, Wang LF, et al. Mixed lineage kinase domain-like protein MLKL causes necrotic membrane disruption upon phosphorylation by RIP3. Mol Cell 2014;53:133–146. doi: 10.1016/j.molcel.2014.03.003.
15. Su L, Quade B, Wang H, Sun L, Wang X, Rizo J. A plug release mechanism for membrane permeation by MLKL. Structure 2014;22:1489–1500. doi: 10.1016/j.str.2014.07.014.
16. Pasparakis M, Vandenabeele P. Necroptosis and its role in inflammation. Nature 2015;517:311–320. doi: 10.1038/nature14191.
17. Kaczmarek A, Vandenabeele P. Necroptosis: the release of damage-associated molecular patterns and its physiological relevance. Immunity 2013;38:209–223. doi: 10.1016/j.immuni.2013.02.003.
18. Mehta SL, Manhas N, Raghubir R. Molecular targets in cerebral ischemia for developing novel therapeutics. Brain Res Rev 2007;54:34–66. doi: 10.1016/j.brainresrev.2006.11.003.

How to cite this article: Liu H, Zhang MZ, Liu YF, Dong XH, Hao Y, Wang YB. Necroptosis was found in a rat ischemia/reperfusion injury flap model. Chin Med J 2019;132:42–50. doi: 10.1097/CM9.0000000000000005